Preparation and Adsorption Performance of Cellulose-graft-Polycaprolactone/Polycaprolactone Porous Material

Lihui Gu, Yunzu Li, Yiqin Yang,* Zhiguo Wang, and Yongcan Jin *

Cellulose-graft-polycaprolactone/polycaprolactone (cell-g-PCL/PCL) was formed by grafting cotton linter pulp with caprolactone *via* ring-opening polymerization catalyzed by $Ti(O\text{-}n\text{-}Bu)_4$. The cell-g-PCL/PCL and polycaprolactone (PCL) were used to prepare porous materials (PMs) using solvent exchange and freeze-drying procedures. The obtained PMs were characterized by their porosity, tensile strength, and thermal stability *via* thermal gravimetric analysis and scanning electron microscopy. The preparation conditions of the cell-g-PCL/PCL PM were optimized based on the characterization results. Compared with PCL PM, cell-g-PCL/PCL PM showed higher porosity and better thermal stability. The adsorptivity of cell-g-PCL/PCL PM for the organic pollutant chlorobenzene was greatly improved compared with that of PCL PM. The adsorption processes of both PMs fit well with the Lagergren pseudo-first-order and pseudo-second-order kinetic models. The results of isothermal adsorption simulation indicated that cell-g-PCL/PCL PM and PCL PM fit better with the Langmuir model and Freundlich model, respectively.

Keywords: Cellulose; Graft; Polycaprolactone (PCL); Porous material; Adsorption; Organic pollutants

Contact information: Jiangsu Co-Innovation Center of Efficient Processing and Utilization of Forest Resources, Nanjing Forestry University, Nanjing 210037, China;
** Corresponding authors: wsfyyq@163.com; jinyongcan@njfu.edu.cn*

INTRODUCTION

Cellulose is the most abundant organic raw material in nature, and it is a cheap, biodegradable, and renewable resource. In addition to its principal use in native form for industries like paper and textile manufacturing, cellulose also constitutes a chemical precursor for the production of organic materials. Cellulose consists of linear polymers of β-1,4-glycosidic-linked D-glucose units. It contains three reactive hydroxyl groups at the C-2, C-3, and C-6 positions of the anhydroglucose unit, which provide cellulose with the possibility of carrying out a variety of chemical reactions. Cellulose derivatives have been obtained through reactions with the hydroxyl groups in cellulose. The use of natural fibers, such as flax, jute, and wood fiber (Riedel and Nickel 1999), instead of traditional reinforcement materials, such as glass fibers, carbon, and talc, provides several advantages, including low density, low cost, specific mechanical properties, and biodegradability (Xiao *et al*. 2012). In spite of the advantages of using cellulose for reinforcement in biocomposites, there are also disadvantages, such as the poor compatibility between the hydrophilic fiber and the hydrophobic polymer (Gradwell *et al*. 2004). When the fiber is chemically modified, the compatibility between the fiber and the polymer can be improved. Cellulose-grafting polymerization is an effective pathway to modify cellulose (Xin *et al*. 2011).

Polycaprolactone (PCL), obtained *via* the ring-opening addition polymerization of caprolactone in the presence of a catalyst, is a simple, linear, aliphatic, and biodegradable

polyester. It has a regular structure and is crystallizable (Major-Gabryś *et al*. 2016). PCL is mechanically compatible with many polymers (Hude *et al*. 2006). Because of its low glass transition temperature, PCL is always blended with polymers that have a higher glass transition temperature, which can plasticize the other components. Substances with low glass transition temperatures are often added to polymers with high glass transition temperature to render them more flexible and to reduce their brittleness (Eastmond 2000). PCL is compatible with various other polymers, which enables the formation of various biodisintegrable blends and use as a biodegradable component (Choi and Park 1996).

As a result of industrialization, organic pollutants have given rise to a serious environmental problem. Organics are used widely in modern industries, but most of them are inert and bio-refractory (Ho *et al*. 2005). Therefore, discharged organic pollutants, particularly in water, must be effectively controlled. Adsorption has been known to be one of the best approaches for wastewater decontamination. The most widely used adsorbent in the adsorptive treatment of wastewater is activated carbon, which is likely to be selective. Therefore, a nonselective adsorbent has become an attractive choice. Many researchers have focused on using cellulose derivatives as a reusable adsorbent to extract organic pollutants from wastewater. The ion-exchange properties of cellulose-grafting copolymers can be applied to remove heavy metal ions from aqueous solutions (Güçlü *et al*. 2003). A number of studies on the removal of heavy metals (Bicak *et al*. 1995; Ahmad *et al*. 2015) and dissolved organic pollutants in aqueous solution (Aloulou *et al*. 2004) using cellulose-based materials have been conducted.

In this work, cell-g-PCL/PCL porous material (cell-g-PCL/PCL PM) and PCL porous material (PCL PM) were prepared using solvent exchange and freeze-drying procedures. The conditions for the preparation of the PMs were optimized to enhance their physical properties. The morphology and thermal features of both PMs were comparatively characterized. The application potential of cell-g-PCL/PCL PM and PCL PM as adsorbents for the adsorption of organic pollutants in wastewater was also investigated.

EXPERIMENTAL

Materials

The cellulose-graft-polycaprolactone (cell-g-PCL) (graft ratio 27.6% to 69.2%) was prepared by grafting cotton linter pulp with caprolactone catalyzed using $Ti(O\text{-}n\text{-}Bu)_4$ *via* ring-opening polymerization, as described in a previous study (Li *et al*. 2015). The polycaprolactone (PCL, M_n 35000 to 45000) was purchased from Shanghai Zi-yi Reagent Co., Ltd., Shanghai, China. All other chemicals were analytical grade, and were purchased from Nanjing Chemical Reagent Co., Ltd., Nanjing, China.

Preparation of cell-g-PCL/PCL PM and PCL PM

PCL PM was prepared using solvent exchange and freeze-drying procedures. The PCL was dispersed in tetrahydrofuran (THF) and sonicated for 10 min to form PCL suspension. The mass fraction of PCL to THF was 5%, 7%, 10%, 14%, 16.7%, or 20% (w/w). The suspension was then transferred to a sealable flask and allowed to rest for 24 h to remove the bubbles. The mixture was frozen, then subsequently soaked in ethanol solution and deionized water. The ethanol solution and deionized water were both refreshed every 8 h for 2 d. Finally, the sample was freeze-dried to obtain PCL PM.

Solvent exchange and freeze-drying procedures was also applied in the preparation

of cell-g-PCL/PCL PM. The cell-g-PCL/PCL was dispersed in THF, and the following steps were consistent with the preparation of PCL PM. The mass fraction of cell-g-PCL/PCL to THF was 6%, 8%, 10%, 14%, 16.7%, or 20% (w/w). The mass ratio of cell-g-PCL to PCL was 1:2, 2:3, 1:1, 3:2, or 2:1 (w:w), and the graft ratio of cell-g-PCL was 27.6%, 36.6%, 44.7%, 58.7%, or 69.2%.

Methods

The porosity of the PM was determined according to the method previously described by Wang *et al*. (2006), and was estimated by the following porosity formula in Eqs. 1 through 3,

$$Porosity\ (\%) = \left(1 - \frac{\rho_v}{\rho}\right) \times 100\% \quad (1)$$

$$\rho = 1/(w_c/\rho_c + w_p/\rho_p) \quad (2)$$

$$\rho_v = m/v \quad (3)$$

where ρ_c is the density of cellulose (1460 kg·m^{-3}), ρ_p is the density of PCL (1100 kg·m^{-3}), w_c and w_p are the weight fractions of cell-g-PCL and PCL in the PM (%), respectively, and m and v are the weight and volume of both PMs (kg, m^3), respectively.

The tensile strength of the PMs (30 mm × 20 mm) was measured using an electronic universal testing machine (UTM-4202, Shenzhen Autostrong, Shenzhen, China) at a crosshead speed of 2 mm·min^{-1}, in accordance with GB/T 1040.5-(2006), using the test conditions for unidirectional fiber-reinforced plastic composites. Scanning electron microscopy (SEM) (JSM-7600, JEOL, Toyko, Japan) was used to characterize the morphology of the PMs. A thermogravimetric analyzer (DTG-60, Shimadzu, Kyoto, Japan) was used to determine the thermal stability of the PMs, with a heating rate of 10 °C·min^{-1} from 30 °C to 600 °C while the apparatus was continually flushed with a nitrogen flow of 50 mL·min^{-1}. All samples were vacuum-dried at 40 °C for 24 h prior to thermal gravimetric analysis (TGA). The prepared chlorobenzene solution was used as simulated wastewater. Solute adsorption experiments were performed in batch conditions by adding PMs into the simulated wastewater (200 mL) with different solute concentrations. The suspensions were stirred (QHJ756B, Xinyi Instrument, Changzhou, China) for 3 h to 4 h at 300 rpm and 25 °C to reach the adsorption equilibrium. The PMs were then isolated *via* centrifugation and washed using the mixed solution of ethanol and deionized water for recycling. The adsorptivities of the organic solute on the PMs were determined using UV spectroscopy (TU-1810, Beijing Puxi General Instrument Co., Ltd., Beijing, China).

RESULTS AND DISCUSSION

Effect of Mass Fraction, Mass Ratio, and Graft Ratio on Porosity and Tensile Strength

Cell-g-PCL/PCL PM (mass ratio of cell-g-PCL to PCL 1:1, graft ratio of cell-g-PCL 69.2%) and PCL PM were prepared with different mass fractions during the process of dispersing in THF. Figure 1 shows the effect of the mass fraction on the porosity and tensile strength of the PMs. The porosity of the PCL PM decreased slowly as the mass fraction increased to 10% and then decreased rapidly as the mass fraction increased beyond 10%. However, the tensile strength curve showed that the tensile strength of the PCL PM

increased with increased mass fraction. The change in porosity (76.2% to 86.2%) was small, which suggested that the mass fraction had a greater effect on the tensile strength. However, the porosity was very low when the mass fraction was 16.7% and 20%. Considering both porosity and tensile strength, a mass fraction of 14% was optimum for the preparation of PCL PM. As shown in Fig. 1, the porosity of the cell-g-PCL/PCL PM decreased slowly with increased mass fraction while the mass fraction was less than 14%. However, it decreased rapidly when the mass fraction was over 14%. The tensile strength of the cell-g-PCL/PCL PM increased with increased mass fraction. These results suggested that a mass fraction of 14% was optimal for the preparation of PMs. The relationship between the measured porosity and the tensile strength of the PMs is shown in Fig. 2. In general, the porosity of cell-g-PCL/PCL PM was always higher than that of PCL PM. Cell-g-PCL/PCL PM exhibited a higher tensile strength than PCL PM at the same porosity, likely because of the higher uniformity of cell-g-PCL/PCL PM.

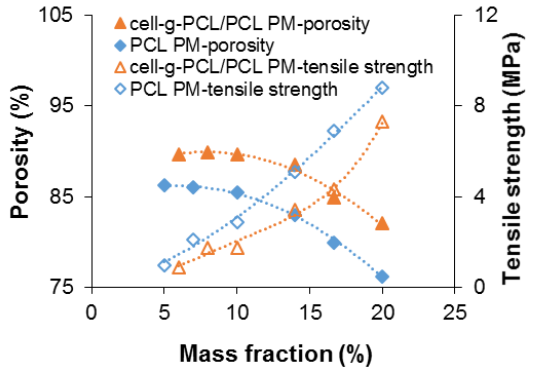

Fig. 1. Effect of mass fraction of cell-g-PCL/PCL and PCL to THF on porosity and tensile strength

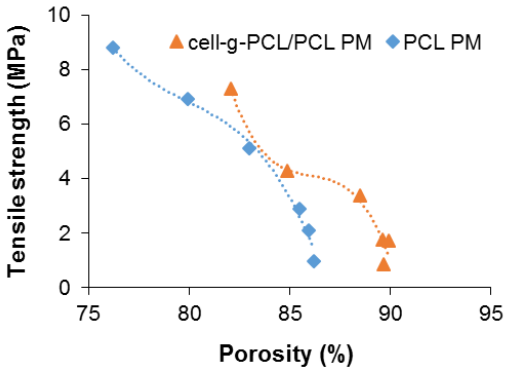

Fig. 2. Tensile strength as a function of porosity of cell-g-PCL/PCL PM and PCL PM

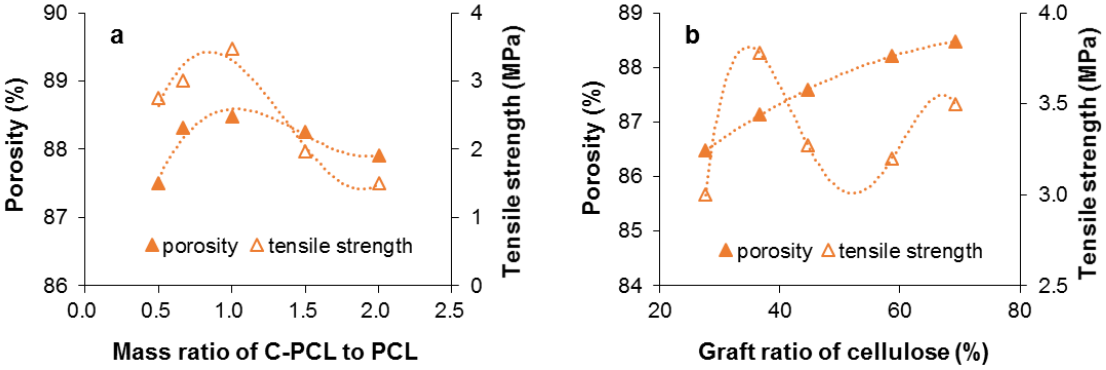

Fig. 3. Porosity and tensile strength of the cell-g-PCL/PCL PM as functions of cell-g-PCL to PCL mass ratio (a: mass fraction 14%, graft ratio of cell-g-PCL 69.2%) and graft ratio of cellulose (b: mass fraction 14%, mass ratio of cell-g-PCL to PCL 1:1)

The effects of mass ratio of cell-g-PCL/PCL to PCL and cellulose graft ratio of cell-g-PCL on PM porosity and tensile strength are shown in Fig. 3. As shown in Fig. 3a, the highest porosity of the material was 88.5%, while the mass ratio of cell-g-PCL to PCL was 1:1. The tensile strength of the PM increased with the mass ratio. It reached the highest value when the mass ratio was 1:1, and decreased sharply when the ratio was over 1. These results implied that a certain amount of cell-g-PCL benefited the uniformity of the prepared

PM, but too much cell-g-PCL in the composite material could destroy the internal crosslinkages, which results in a decreased tensile strength. As can be seen in Fig. 3b, the porosity of the PM increased slowly with an increased graft ratio. A higher graft ratio of cell-g-PCL appeared to improve the porosity. This result could be explained by the fact that the high graft ratio improved the compatibility between cell-g-PCL and PCL. However, the changes in tensile strength were irregular.

Structural Characteristics of Cell-g-PCL/PCL PM and PCL PM

Scanning electron microscopy and TGA were used to study the surface morphology and thermal stability of the cell-g-PCL/PCL PM (mass ratio of cell-g-PCL to PCL 1:1, graft ratio of cell-g-PCL 69.2%, mass fraction to THF 10%) and PCL PM (mass fraction to THF 10%), as shown in Figs. 4 and 5. Compared with PCL PM, the cell-g-PCL/PCL PM showed higher porosity. The PCL PM was shown as a large and perfect spherulite composed of numerous linear PCL polymers. The structure of the PCL PM was relatively compact due to the high crystallization ability of PCL (Yuan *et al*. 2006). The morphology of the cell-g-PCL/PCL PM, made up of a profusion of platelets 1 μm in width, was rather different from that of the PCL PM. This difference could have been explained by the fact that the crosslinking of cell-g-PCL with PCL hindered the crystallization of PCL when PCL was composited with cell-g-PCL.

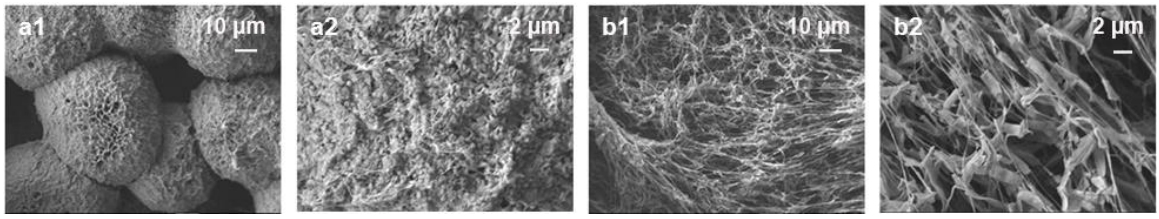

Fig. 4. SEM images of PCL PM (a1, a2) and cell-g-PCL/PCL PM (b1, b2)

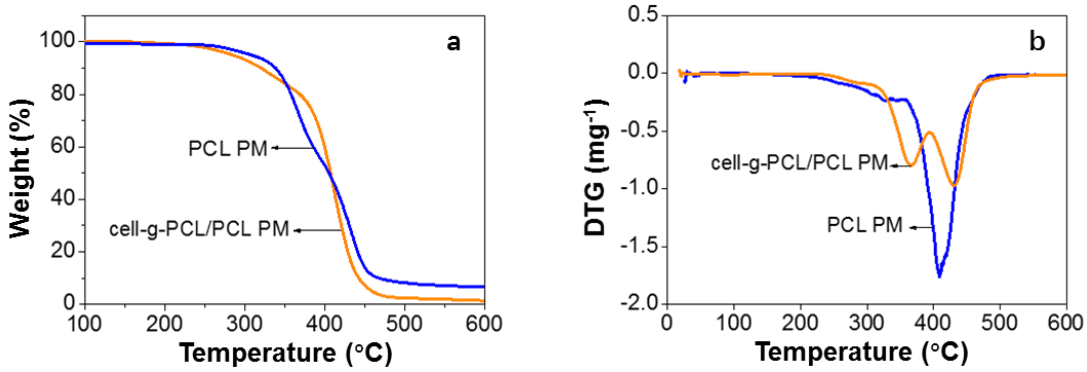

Fig. 5. TGA (a) and DTG (b) curves of cell-g-PCL/PCL PM and PCL PM

As shown in Fig. 5, the decomposition temperature of the PCL PM was 417 °C, while that of the cell-g-PCL/PCL PM was 369 °C and 436 °C. The thermal decomposition of cell-g-PCL/PCL underwent two stages. The degradation of cellulose continued up to 369 °C in the first stage. The degradation of PCL started at 369 °C, and a residue of 15 wt.% remained after heating to 436 °C. These results suggested that compared with the PCL PM, the cell-g-PCL/PCL PM showed a higher thermal stability. The increased thermal stability of the cell-g-PCL/PCL PM could have been attributed to the intermolecular force of the material increasing with the introduction of cell-g-PCL.

Adsorption Properties of Cell-g-PCL/PCL PM and PCL PM

The adsorption properties of the prepared cell-g-PCL PM (mass fraction 14%, graft ratio of cell-g-PCL 69.2%, ratio of cell-g-PCL to PCL 1:1, porosity 88.5%) and PCL PM (mass fraction 14%, porosity 83%) were investigated. Chlorobenzene (3.0 mmol·L^{-1}) was used as an organic pollutant to investigate the adsorption ability of the PMs at 25 °C. As shown in Fig. 6a, the adsorption increased rapidly in a short period of time, and the adsorption processes attained equilibrium after approximately120 min for both PMs. This result was explained by the fact that in the beginning of the process, the surface area and the availability of adsorption sites were relatively high, and the organic pollutant was easily adsorbed. The total available adsorption sites then became limited, which resulted in a decrease of the adsorption rate. Finally, the adsorption could no longer increase as a result of the saturation of adsorption (EI-Latif *et al*. 2013). The maximum adsorption onto the cell-g-PCL/PCL PM (14.13 mmol·g^{-1}) was approximately 80% higher than chlorobenzene was adsorbed onto the PCL PM (7.91 mmol·g^{-1}). The effect of initial concentration of chlorobenzene on the adsorption of the cell-g-PCL/PCL PM and PCL PM with an adsorption time of 180 min at 25 °C is shown in Fig. 6b. The isotherms displayed a rapid increase, followed by a saturation plateau, at an initial solution concentration of approximately 3.0 mmol·L^{-1}. At the plateau, the maximum adsorption onto the cell-g-PCL/PCL PM and PCL PM was 14.28 mmol·g^{-1} and 8.36 mmol·g^{-1}, respectively. These results showed that the adsorption ability of the organic pollutant onto the cell-g-PCL/PCL PM was greatly increased compared with that of the PCL PM. The maximum adsorption of chlorobenzene onto the cell-g-PCL/PCL PM was 14.21 mmol·g^{-1} (the average value of two maximum absorption data).

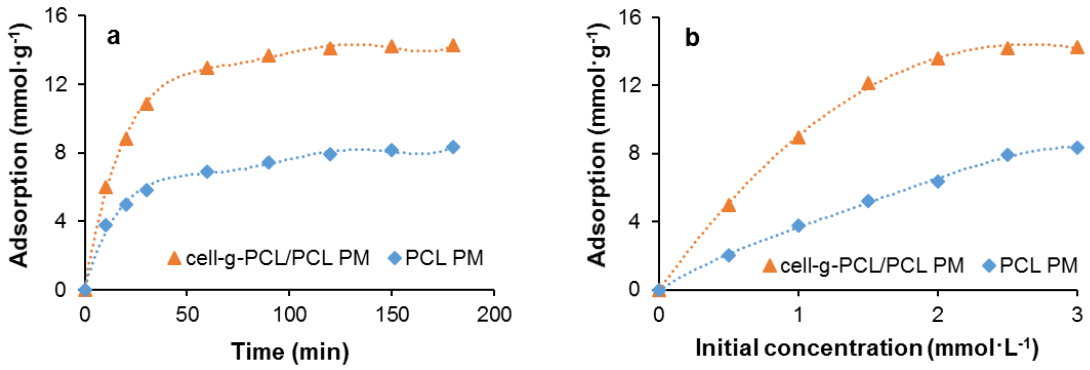

Fig. 6. Adsorption of chlorobenzene onto the cell-g-PCL/PCL PM and PCL PM as a function of adsorption time (a) and chlorobenzene initial concentration (b)

Adsorption kinetics

Three simplified kinetic models were discussed to identify the kinetics of the adsorption of chlorobenzene (3 mmol·L^{-1}) onto the cell-g-PCL/PCL PM and PCL PM at 25 °C. The pseudo-first-order reaction equation is one of the most widely used to describe the adsorption of an adsorbate from the liquid phase (Ho and McKay 1999). The pseudo-first-order rate is represented as Eq. 4,

$$ln(q_e - q_t) = lnq_e - (k_f/2.303)t \quad (4)$$

where q_e and q_t are the amount (mg·g^{-1}) of chlorobenzene on the adsorbent at equilibrium and at time t (min), respectively, and k_f is the rate constant of pseudo-first-order adsorption (min^{-1}). The values of q_e and k_f for the pseudo-first-order kinetic model were determined

from the intercept and slope of the plot of $ln(q_e-q_t)$ *versus t*, as shown in Fig. 7a. The calculated results of the pseudo-first-order rate equation are given in Table 1.

The kinetics of adsorption can be represented by the pseudo-second-order rate as Eq. 5 (Ho and McKay 1999),

$$t/q_t = 1/(k_s q_e^2) + 1/q_e t \quad (5)$$

where q_e and q_t have the same meaning as previously mentioned, k_s is the rate constant of the pseudo-second-order adsorption ($mg \cdot g^{-1} \cdot s^{-1}$). The values of q_e and k_s were determined from the intercept and slope of the plot of t/q_t *versus t*, as shown in Fig. 7b. The calculated results of the pseudo-second-order rate equation are given in Table 1.

The kinetic data was further analyzed using the intraparticle diffusion model Eq. 6 based on the theory proposed by Weber and Morris (1963), which is represented as,

$$q_t = k_{id} t^{1/2} + C \quad (6)$$

where q_t is the amount of chlorobenzene ($mg \cdot g^{-1}$) on the adsorbent at equilibrium and k_{id} is the rate constant of the intraparticle diffusion parameter ($mg \cdot g^{-1} min^{-1/2}$), *C* is the boundary layer thickness ($mg \cdot g^{-1}$). The values of k_{id} and *C* were determined from the slope and intercept of the plot q_t *versus* $t^{1/2}$, as shown in Fig. 7c. The calculated results of the Weber and Morris model are given in Table 1.

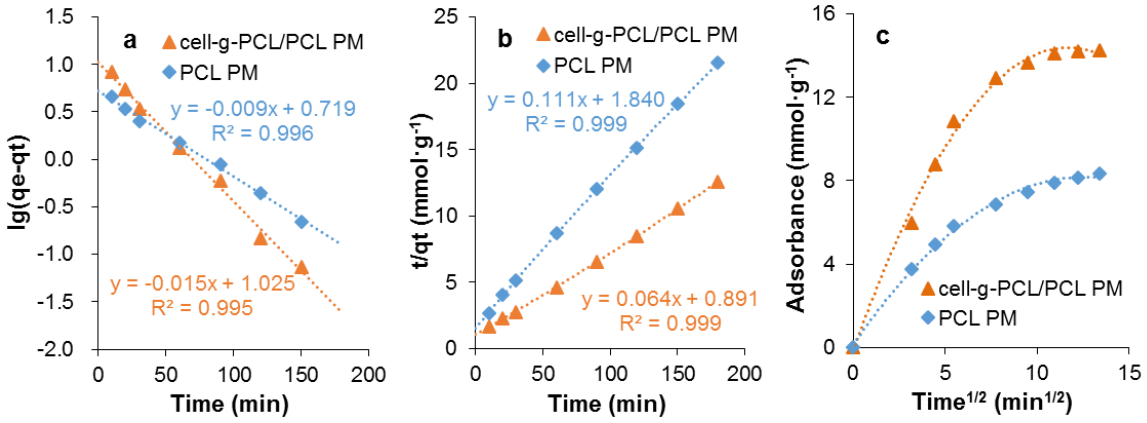

Fig. 7. Lagergren pseudo first-order kinetic model (a); Lagergren pseudo second-order kinetic model (b); and Weber and Morris intragranular diffusive model (c)

Table 1. Parameters of Three Kinetic Models

Sample	Pseudo-first-order			Pseudo-second-order			Weber and Morris		
	q_e ($mg \cdot g^{-1}$)	k_f (min^{-1})	R^2	q_e ($mg \cdot g^{-1}$)	k_s ($mg \cdot g^{-1} \cdot s^{-1}$)	R^2	k_{id} ($mg \cdot g^{-1} \cdot min^{-1/2}$)	*C*	R^2
PCL PM	5.2	0.021	0.996	9.0	0.006	0.999	0.6	1.7	0.889
Cell-g-PCL/PCL PM	10.6	0.034	0.995	15.6	0.005	0.999	1.0	3.1	0.851

The data show that the values of R^2 for the PMs obtained from pseudo-first-order and pseudo-second-order models were as high as 0.995 to 0.999. Hence, the kinetics of adsorption of chlorobenzene onto the cell-g-PCL/PCL PM and PCL PM fit well with both the Lagergren pseudo-first-order and pseudo-second-order kinetic models, but the adsorption processes were not in conformity with the Weber and Morris intraparticle diffusion model. The results revealed that the adsorption process was dominated by the concentration of chlorobenzene solution. From Fig. 7c, it can be concluded that the plot of

q_t *versus* $t^{1/2}$ was not a straight line passing through the origin, suggesting that intraparticle diffusion was not the only mechanism for the overall adsorption process, which also included surface diffusion (Soheir *et al.* 2014).

Adsorption isotherms

In this study, adsorption of chlorobenzene onto cell-g-PCL PM and PCL PM with an adsorption time of 180 min at 25 °C was modeled using isotherm models.

The Langmuir adsorption isotherm model is based on an assumption that the adsorption occurs at specific homogeneous sites within the adsorbent (Al-Asheh *et al.* 2000). The Langmuir isotherm model (Eq. 7) is expressed as,

$$C_e/q_e = 1/(Q_m\, k_L) + C_e/Q_m \quad (7)$$

where C_e is the equilibrium concentration of the adsorbate (mmol·L^{-1}), q_e is the amount of adsorbate per unit mass of adsorbent (mmol·g^{-1}), Q_m is the maximum adsorption capacity (mmol·g^{-1}), and k_L is the Langmuir constant related to the energy of adsorption (L·mmol^{-1}). The values of Q_m and k_L (Table 2) were calculated from the slope and intercept of the plot of C_e/q_e *versus* C_e, which is shown in Fig. 8a.

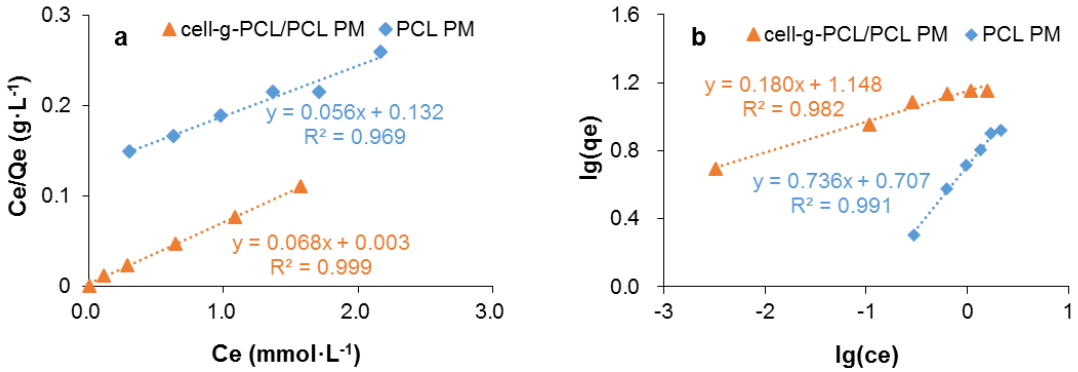

Fig. 8. Langmuir (a) and Freundlich (b) linear fitting of the isothermal adsorption curve of chlorobenzene onto cell-g-PCL PM and PCL PM

Table 2. Parameters of Different Isothermal Adsorption Models

Sample	Langmuir			Freundlich		
	Q_m (mmol·g^{-1})	K_L (mmol·L^{-1})	R^2	K_F ([mg·g^{-1}][L·mg^{-1}]$^{1/n}$)	n	R^2
PCL PM	17.9	0.4	0.969	5.1	1.4	0.991
Cell-g-PCL/PCL PM	14.6	22.8	0.999	14.1	5.6	0.982

The Freundlich isotherm model describes adsorption onto heterogeneous surfaces with interaction between the adsorbed molecules (Al-Asheh *et al.* 2000). The well-known linear of the Freundlich model, Eq. 8, is expressed as follows,

$$\lg q_e = lg k_F + 1/n\, lg C_e \quad (8)$$

where C_e and q_e have the same meaning as previously mentioned, k_F ([mg·g^{-1}][L·mg^{-1}]$^{1/n}$) is the Freundlich constant, and $1/n$ is an empirical constant. Figure 8b shows the plot of $\lg q_e$ *versus* $lg C_e$, giving linear relations. The variable n represents the effect of concentration on adsorptivity. The values of k_F and n were calculated, and the results are tabulated in Table 2.

The R^2 of the cell-g-PCL/PCL PM for the Langmuir adsorption isotherm model was 0.999. The Q_m value of the cell-g-PCL/PCL PM calculated by the Langmuir isotherm model (14.61 mmol·g^{-1}) was close to the experimental value (14.21 mmol·g^{-1}) with the same adsorption conditions. These results indicated that the cell-g-PCL/PCL PM fit better with the Langmuir adsorption isotherm. From Table 2, the *n* value of the cell-g-PCL/PCL PM was greater than that of the PCL PM, which indicated that the adsorptivity of the cell-g-PCL/PCL PM was higher than that of the PCL PM. The R^2 of the PCL PM for the Freundlich adsorption isotherm model (0.991) showed that the PCL PM fit well with the Freundlich model.

CONCLUSIONS

1. Cell-g-PCL/PCL PM was prepared *via* a solvent exchange method. The parameters, such as mass fraction, mass ratio of cell-g-PCL to PCL, and graft ratio of cell-g-PCL, had significant effects on the porous structure of the materials.
2. A mass fraction of 14%, mass ratio of 1:1, and higher graft ratio were optimum for the preparation of the cell-g-PCL/PCL PM. The cell-g-PCL/PCL PM had higher porosity and better thermal stability than the PCL PM.
3. The adsorptivity of organic pollutant onto the cell-g-PCL/PCL PM was greatly improved compared with that of the PCL PM, which showed the cell-g-PCL/PCL material has potential for the removal of organic pollutant. The maximum adsorptivity of chlorobenzene onto the cell-g-PCL/PCL PM was 14.21 mmol·g^{-1}.
4. The adsorption processes of both PMs fit well with the Lagergren pseudo-first-order and pseudo-second-order kinetic models. The results of isothermal adsorption simulation indicated that the cell-g-PCL/PCL PM and PCL PM fit better with the Langmuir model and the Freundlich model, respectively.

ACKNOWLEDGMENTS

The authors are grateful for the support of Foundation of Jiangsu Students' Platform for Innovation and Entrepreneurship, China (201410298055Z), Jiangsu Provincial Key Lab of Pulp and Paper Science and Technology, China (201321), and Priority Academic Program Development of Jiangsu Higher Education Institutions, China.

REFERENCES CITED

Ahmad, M., Ahmed, S., Swami, B. L., and Ikram, S. (2015). "Adsorption of heavy metal ions: Role of chitosan and cellulose for water treatment," *Int. J. Pharmacogn.* 2(6), 280-289. DOI: 10.13040/UPSR.0975-8232.UP.2(6).280-89

Aloulou, F., Boufi, F., and Beneventi, D. (2004). "Adsorption of organic compound onto polyelectrolyte immobilized-surfactant aggregates onto cellulosic fibers," *J. Colloid Interf. Sci.* 280(2), 350-358. DOI: 10.1016/j.jcis.2004.08.008

Al-Asheh, S., Banat, F., Al-Omari, R., and Duvnjak, Z. (2000). "Predictions of binary sorption isotherms for the sorption of heavy metals of pine bark using single isotherm

data," *Chemosphere* 41(7), 659-665. DOI: 10.1016/S0045-6535(99)00497-X

Bicak, N., Sherrington, D. C., and Senkal, B. F. (1995). "Mercury sorption by 'non-functional' crosslinked polyacrylamides," *React. Funct. Polym.* 27(3), 155-161. DOI: 10.1016/1381-5148(95)00048-K

Choi, E. J., and Park, J. K. (1996). "Study on biodegradability of PCL/SAN blend using composting method," *Polym. Degrad. Stabil.* 52(3), 321-326. DOI: 10.1016/0141-3910(96)00032-8

Eastmond, G. C. (2000). "Poly (ε-caprolactone) blends," *Adv. Polym. Sci.* 149(10), 59-222. DOI: 10.1007/3-540-48838-3-2

EI-Latif, M. M. A., Ibrahim, A. M., Showman, M. S., and Hamide, R. R. A. (2013). "Alumina/iron oxide nano composite for cadmium ions removal from aqueous solution," *Int. J. Nonferr. Met.* 2(2), 47-62. DOI: 10.4236/ijnm.2013.22007

GB/T 1040.5-2006 (2008). "Plastics – Determination of tensile properties – Part 5: Test conditions for unidirectional fiber-reinforced plastic composites," Standardization Administration of China, Beijing, China.

Gradwell, S., Reneckar, S., Esker, A., Heinze, T., Gatenholm, P., Vaca-Garcia, C., and Glasser, W. (2004). "Surface modification of cellulose fibres: Towards wood composites by biomimetics," *C. R. Biol.* 327(9-10), 945-953. DOI: 10.1016/j.crvi.2004.07.015

Güçlü, G., Gürdağ, G., and Özgümüş, S. (2003). "Competitive removal of heavy metal ions by cellulose graft copolymers," *J. Appl. Polym. Sci.* 90(8), 2034-2039. DOI: 10.1002/app.12728

Ho, Y. S., Chiang, T. H., and Hsueh, Y. M. (2005). "Removal of basic dye from aqueous solution using tree fern as a biosorbent," *Process Biochem.* 40(1), 119-124. DOI: 10.1016/j.procbio.2003.11.035

Ho, Y. S., and McKay, G. (1999). "Pseudo-second order model for sorption processes," *Process Biochem.* 34(5), 451-465. DOI: 10.1016/S0032-9592(98)00112-5

Hude, M. S., Przal, L. T., Misra, M., and Mohanty, A. K. (2006). "Wood-fiber-reinforced poly (lactic acid) composites: Evaluation of the physicomechanical and morphological properties," *J. Appl. Polym. Sci.* 102(5), 4856-4869. DOI: 10.1002/app.24829

Li, Y. Z., Yang, Y. Q., Yang, Q. W., Gu, L. H., and Wang, Z. G. (2015). "Catalytic grafting of cellulose fibers with polycaprolactone by tetrabutyl titanate," *J. Nanjing Forest. Univ.* 39(3), 113-118. DOI: 10.1021/bm060178z

Major-Gabryś, K., Grabarczyk, A., Dobosz, S. T., and Jakubski, J. (2016). "New bicomponent binders for foundry moulding sands composed of phenol-furfuryl resin and polycaprolactone," *Metalurgija* 55(3), 385-387.

Riedel, U., and Nickel, J. (1999). "Natural fibre-reinforced biopolymers as construction materials-new discoveries," *Angew. Makromol. Chem.* 272(1999), 34-40. DOI: 10.1002/(SICI)1522-9505(19991201)272:13.0.CO;2-H

Soheir, K., Mona, S., Nady, F., and Amina, A. (2014). "Effect of physical and chemical activation on the removal of hexavalent chromium ions using palm tree branches," *ISRN Environ. Chem.* 60(4), 1-10. DOI: 10.1155/2014/705069

Wang, K. M., Li, S. R., and Guo, J. (2006). "Study on preparation of scaffold for tissue engineering by thermally induced phase separation technique," *Chem. Biol. Eng.* 23(1), 1-3. DOI: 10.3969/j.issn.1672-5425.2006.01.001

Weber, W. J., and Morris, J. C. (1963). "Kinetics of adsorption on carbon from aqueous solutions," *J. Sanit. Eng. Div.* 89, 31-60.

Xiao, A., Yuan, T. Q., Cao, H. C., Lin, D., Shen, Y., He, J., and Wang, B. (2012). "Synthesis and characterization of cellulose-graft-poly (L-lactide) *via* ring-opening polymerization," *BioResources* 7(2), 1748-1759. DOI: 10.15376/biores.7.2.1748-1759

Xin, T. T., Yuan, T. Q., Xiao, S., and He, J. (2011). "Synthesis of cellulose-graft-poly (methyl methacrylate) *via* homogeneous ATRP," *BioResources* 6(3), 2941-2953. DOI: 10.15376/biores.6.3.2941-2953

Yuan, W. Z., Yuan, J. Y., Zhang, F. B., and Xie, X. M. (2006). "Syntheses, characterization and *in vitro* degradation of ethyl cellulose-graft-poly (ε-caprolactone)-block-poly (L-lactide) copolymers by sequential ring-opening polymerization," *Biomacromolecules* 8(4), 1101-1108. DOI: 10.1021/bm0610018

Article submitted: January 24, 2017; Peer review completed: May 11, 2017; Revisions accepted: June 3, 2017; Published: June 16, 2017.
DOI: 10.15376/biores.12.3.5539-5549